Online Physics-Informed Learning-Based Identification: Application to Adaptive MTPA Control of Synchronous Machines ⋆

Seunghun Jang * **Kyunghwan Choi** *

* *Korea Advanced Institute of Science and Technology (KAIST), Daejeon 34051, South Korea (e-mail: {shjang7071, kh.choi}@kaist.ac.kr)*

Abstract: Machine parameters such as flux linkages and inductances play a key role in achieving optimal torque control of synchronous machines (SMs). However, it is challenging to identify these parameters online based on the SM model, which has complex and nonlinear characteristics. A fully connected feedforward neural network (NN) is a promising candidate owing to its capability to approximate complex nonlinear functions. Therefore, this study proposes an online physics-informed learning framework for identifying the parameters of SMs using an NN. The proposed method enables the NN-modeled flux linkages and inductances to be learned online in compliance with the governing physical laws of SMs. Consequently, the NN can more effectively capture the nonlinear characteristics of SMs within the constraints imposed by these governing physical laws. The learned parameters can be employed as online estimators and applied to online MTPA control. As a result, the effectiveness of the proposed method is validated through simulations conducted on a 35-kW interior permanent magnet synchronous motor (IPMSM) drive.

Keywords: Online identification, physics-informed learning, synchronous machines, flux linkage estimation, adaptive MTPA control

1. INTRODUCTION

1.1 Motivation and Background

Synchronous machines (SMs) are widely used in various industrial applications, where high efficiency and high torque performance are essential. In particular, the drive efficiency of SMs is influenced by torque control performance. Accordingly, numerous advanced torque control strategies have been investigated, including generalized model predictive torque control (GMPTC) Choi et al. (2025), which directly determines the voltage input under operational constraints; optimal feedforward current control Monzen and Hackl (2025); advanced MPC-based frameworks Rodriguez et al. (2022); and finite-control-set MPC approaches Ahmed et al. (2017), all of which require accurate knowledge of machine parameters such as the flux linkage and inductances of SMs.

There are two approaches to obtaining machine parameters for SMs, which can be classified into (i) offline identification and (ii) online identification. In offline approaches, flux linkage and inductance maps are typically built as lookup tables (LUTs) using analytical machine models, finite-element analysis (FEA), or extensive steady-state experiments over the full operating range. Although widely adopted, this process is time-consuming and costly, and the resulting maps cannot accommodate parameter variations induced by temperature changes, demagnetization, or aging. These limitations underscore the need for online estimation methods capable of continuously adapting machine parameters to varying operating conditions.

In the online approach, several studies have estimated the stator flux linkages by integrating the SM voltage equations in the α–β frame. These include a Gopinath-style observer Lee et al. (2011), which neglects cross-coupling effects, and the method in Yoo and Sul (2009), which compensates for such coupling only under steady-state conditions. However, these voltage-model-based approaches require high-pass filtering for DC-offset removal, which distorts low-frequency components and limits the accuracy of flux estimation under dynamic operating conditions.

More advanced observer-based estimators have recently been proposed, including the disturbance-observer-based flux linkage estimator (DOBFLE) Monzen et al. (2023), the extended-state-observer-based estimator (ESOFLE) Jang et al. (2024), and the integration-error-estimation linear observer in Jang and Choi (2023). These methods offer improved flux estimation performance but remain sensitive to nominal parameter deviations, leading to degraded transient performance.

Despite these advancements, the aforementioned studies still struggle with accurate flux estimation and do not provide inductance information, which leads to inherent limitations in achieving optimal torque control.

Furthermore, several studies have explored data-driven online approaches for modeling the machine's torque-

⋆ This work was supported in part by the National Research Foundation of Korea (NRF) grant funded by the Korea government (MSIT) (RS-2025-00554087).

(*Corresponding author: Kyunghwan Choi*)

generation characteristics. In Brosch et al. (2021), a recursive least squares (RLS) algorithm is used to estimate the differential inductances and torque required for torque control of synchronous machines; however, the RLS update is not free from rank deficiency across all operating regions, and the flux obtained by integrating the inductance estimates also suffers from integration errors, making it difficult to guarantee accurate torque estimation performance. In addition, Ortombina et al. (2019) employs a radial basis function (RBF) network to learn local maximum torque per ampere (MTPA) characteristics, but the training is restricted to steady-state conditions and does not account for flux dynamics.

1.2 Contributions

The aforementioned studies reveal that accurately estimating the flux required for optimal torque control of SMs is difficult under transient conditions, and that reliable inductance estimation also has fundamental limitations, such as rank deficiency in the RLS update. To address these issues, this study proposes an online physics-informed model learning framework for parameter identification of SMs. The key idea is to model the stator flux linkages and differential inductances using a fully connected NN and to learn this model online in compliance with the governing physical laws of SMs. The NN-based flux linkages and inductances estimated online can be directly used in the MTPA control strategy to achieve adaptive optimal torque control. The main contributions of this paper are summarized as follows:

1) A fully-connected feedforward NN model is introduced to model the stator flux linkages and differential inductances, enabling accurate approximation of their nonlinear dependence on the stator currents.
2) The governing physical laws of SMs are embedded in the online physics-informed learning process, and the learning rules are derived via a residual-minimization approach based on the gradient descent method.
3) The flux–inductance estimates learned by the NN are utilized in the MTPA control to achieve adaptive optimal torque control.

2. PRELIMINARIES

2.1 SM Model

The electrical model of SM in the rotating d-q reference frame is given by

$$\frac{\mathrm{d}}{\mathrm{d}t}\boldsymbol{\psi}_{\mathrm{s}}^{dq}\left(\boldsymbol{i}_{\mathrm{s}}^{dq}\right) = \boldsymbol{v}_{\mathrm{s}}^{dq} - \mathrm{R}_{\mathrm{s}}\boldsymbol{i}_{\mathrm{s}}^{dq} - \omega_{\mathrm{r}}\mathbf{J}\boldsymbol{\psi}_{\mathrm{s}}^{dq}\left(\boldsymbol{i}_{\mathrm{s}}^{dq}\right), \tag{1a}$$

$$T_{\mathrm{e}} = 1.5\mathrm{P}\left(\boldsymbol{i}_{\mathrm{s}}^{dq\top}\mathbf{J}\boldsymbol{\psi}_{\mathrm{s}}^{dq}\right), \tag{1b}$$

with the stator flux linkage vector $\boldsymbol{\psi}_{\mathrm{s}}^{dq} := \left(\psi_{\mathrm{s}}^{d}\ \psi_{\mathrm{s}}^{q}\right)^{\top}$, the stator voltage vector $\boldsymbol{v}_{\mathrm{s}}^{dq} := \left(v_{\mathrm{s}}^{d}\ v_{\mathrm{s}}^{q}\right)^{\top}$, the stator current vector $\boldsymbol{i}_{\mathrm{s}}^{dq} := \left(i_{\mathrm{s}}^{d}\ i_{\mathrm{s}}^{q}\right)^{\top}$, the stator resistance R_{s}, the electrical rotor speed ω_{r}, the rotation matrix $\mathbf{J} := \begin{bmatrix}0 & -1\\ 1 & 0\end{bmatrix}$, the electrical torque T_{e}, and the number of pole pairs P.

In general, when magnetic saturation and cross-coupling effects are considered, the flux linkage becomes a nonlinear function of the stator current vector, (i.e., $\boldsymbol{\psi}_{\mathrm{s}}^{dq}(\boldsymbol{i}_{\mathrm{s}}^{dq})$). Its time derivative can be expressed by applying the chain rule with respect to the stator current $\boldsymbol{i}_{\mathrm{s}}^{dq}$ as

$$\frac{\mathrm{d}}{\mathrm{d}t}\boldsymbol{\psi}_{\mathrm{s}}^{dq}(\boldsymbol{i}_{\mathrm{s}}^{dq}) = \underbrace{\frac{\partial\boldsymbol{\psi}_{\mathrm{s}}^{dq}(\boldsymbol{i}_{\mathrm{s}}^{dq})}{\partial\boldsymbol{i}_{\mathrm{s}}^{dq}}}_{=:\mathbf{L}_{\mathrm{s}}^{dq}(\boldsymbol{i}_{\mathrm{s}}^{dq})}\frac{\mathrm{d}}{\mathrm{d}t}\boldsymbol{i}_{\mathrm{s}}^{dq}, \tag{2}$$

with the differential inductance matrix

$$\mathbf{L}_{\mathrm{s}}^{dq}(\boldsymbol{i}_{\mathrm{s}}^{dq}) := \begin{bmatrix}\mathrm{L}_{\mathrm{s}}^{dd} & \mathrm{L}_{\mathrm{s}}^{dq}\\ \mathrm{L}_{\mathrm{s}}^{qd} & \mathrm{L}_{\mathrm{s}}^{qq}\end{bmatrix}, \tag{3}$$

where $\mathrm{L}_{\mathrm{s}}^{dd} := \frac{\partial\psi_{\mathrm{s}}^{d}}{\partial i_{\mathrm{s}}^{d}}$ and $\mathrm{L}_{\mathrm{s}}^{qq} := \frac{\partial\psi_{\mathrm{s}}^{q}}{\partial i_{\mathrm{s}}^{q}}$ denote the d- and q-axis self differential inductances, and $\mathrm{L}_{\mathrm{s}}^{dq} := \frac{\partial\psi_{\mathrm{s}}^{d}}{\partial i_{\mathrm{s}}^{q}}$ and $\mathrm{L}_{\mathrm{s}}^{qd} := \frac{\partial\psi_{\mathrm{s}}^{q}}{\partial i_{\mathrm{s}}^{d}}$ denote the mutual differential inductances, respectively.

Substituing (2) into (1a) results in the PDE model, i.e.,

$$\frac{\partial\boldsymbol{\psi}_{\mathrm{s}}^{dq}(\boldsymbol{i}_{\mathrm{s}}^{dq})}{\partial\boldsymbol{i}_{\mathrm{s}}^{dq}}\frac{\mathrm{d}}{\mathrm{d}t}\boldsymbol{i}_{\mathrm{s}}^{dq} = \boldsymbol{v}_{\mathrm{s}}^{dq} - \mathrm{R}_{\mathrm{s}}\boldsymbol{i}_{\mathrm{s}}^{dq} - \omega_{\mathrm{r}}\mathbf{J}\boldsymbol{\psi}_{\mathrm{s}}^{dq}(\boldsymbol{i}_{\mathrm{s}}^{dq}), \tag{4}$$

which serves as the fundamental governing equation for the online physics-informed learning of the flux linkages and differential inductances (see Section 3.2 for further details).

In this work, the following assumptions are made for the SM model:

- The stator resistance R_{s} is assumed to be known.
- The stator current vector $\boldsymbol{i}_{\mathrm{s}}^{dq}$ and the electrical rotor speed ω_{r} are measurable.
- Inverter nonlinearities and iron losses (including eddy-current and hysteresis effects) are considered negligible.

2.2 Online MTPA Control

The efficient operation of SMs can be achieved by minimizing copper losses while satisfying a torque requirement, which is known as the maximum torque per ampere (MTPA) strategy. In the MTPA region, the nonlinear constrained optimization problem is formulated as

$$\min_{\boldsymbol{i}_{\mathrm{s}}^{dq}} \frac{1}{2}\left\|\boldsymbol{i}_{\mathrm{s}}^{dq}\right\|^{2} \tag{5a}$$

$$\text{s.t.}\quad T_{\mathrm{e}} - T_{\mathrm{e}}^{*} = 0, \tag{5b}$$

where T_{e}^{*} is the desired torque command. To solve (5), the Lagrangian function is defined as

$$\mathcal{L}(\boldsymbol{i}_{\mathrm{s}}^{dq},\lambda) := \frac{1}{2}\left\|\boldsymbol{i}_{\mathrm{s}}^{dq}\right\|^{2} + \lambda\left(1.5\mathrm{P}\left(\boldsymbol{i}_{\mathrm{s}}^{dq\top}\mathbf{J}\boldsymbol{\psi}_{\mathrm{s}}^{dq}\right) - T_{\mathrm{e}}^{*}\right), \tag{6}$$

where λ is the Lagrange multiplier for the torque equality constraint. The optimal solutions ($\boldsymbol{i}_{\mathrm{s}}^{dq*}$ and λ^{*}) can be obtained by minimizing the Lagrangian with respect to $\boldsymbol{i}_{\mathrm{s}}^{dq}$ and maximizing it with respect to λ, following a simplified primal–dual gradient update inspired by the augmented Lagrangian approach in Choi et al. (2025), as

$$\boldsymbol{i}_{\mathrm{s}}^{dq*} = \boldsymbol{i}_{\mathrm{s}}^{dq} - \alpha\nabla_{\boldsymbol{i}_{\mathrm{s}}^{dq}}\mathcal{L}(\boldsymbol{i}_{\mathrm{s}}^{dq},\lambda), \tag{7a}$$

$$\lambda^{*} = \lambda + \beta\nabla_{\lambda}\mathcal{L}(\boldsymbol{i}_{\mathrm{s}}^{dq},\lambda), \tag{7b}$$

with

$$\nabla_{\boldsymbol{i}_{\mathrm{s}}^{dq}}\mathcal{L}(\boldsymbol{i}_{\mathrm{s}}^{dq},\lambda) = \boldsymbol{i}_{\mathrm{s}}^{dq} + 1.5\lambda\mathrm{P}\left(\mathbf{J}\boldsymbol{\psi}_{\mathrm{s}}^{dq} - \mathbf{L}_{\mathrm{s}}^{dq\top}\mathbf{J}\boldsymbol{i}_{\mathrm{s}}^{dq}\right), \tag{8a}$$

$$\nabla_{\lambda}\mathcal{L}(\boldsymbol{i}_{\mathrm{s}}^{dq},\lambda) = 1.5\mathrm{P}\left(\boldsymbol{i}_{\mathrm{s}}^{dq\top}\mathbf{J}\boldsymbol{\psi}_{\mathrm{s}}^{dq}\right) - T_{\mathrm{e}}^{*}, \tag{8b}$$

where $\alpha, \beta > 0$ are the step sizes for the primal and dual updates, respectively. This update drives the Lagrangian along the proper descent–ascent directions and thereby satisfies the KKT (Karush–Kuhn–Tucker) optimality conditions at the stationary point.

Solving the MTPA problem (5) requires accurate flux linkage and differential inductance information to compute a reliable gradient direction in (8). In practice, these quantities are typically obtained from pre-identified lookup tables constructed from FEA-based analysis. However, such maps may deviate from their nominal values as a result of parameter variations caused by temperature fluctuations, magnetic saturation, and long-term degradation, thereby limiting the applicability and robustness of LUT-based MTPA control. These limitations require an online parameter estimation mechanism capable of adapting to the actual machine characteristics.

3. ONLINE PHYSICS-INFORMED FLUX MODEL LEARNING

As discussed in Section 2.2, it is necessary to estimate key machine parameters—such as the flux linkage $\boldsymbol{\psi}_{\mathrm{s}}^{dq}$ and differential inductance $\mathbf{L}_{\mathrm{s}}^{dq}$—online to achieve optimal torque control. However, directly identifying these quantities online from the SM model (1) is challenging due to their strong nonlinear dependence on the stator current vector $\boldsymbol{i}_{\mathrm{s}}^{dq}$ and the limited number of explicit equations available for parameter identification.

To overcome these challenges, we develop an online physics-informed learning framework in which the governing SM equations are embedded as physical constraints, enabling the neural network (NN) to learn the model directly from the underlying machine physics. First, a fully-connected feedforward NN that represents the complex nonlinear characteristics of the machine is introduced in Section 3.1, and this NN structure is then used to model the flux linkage and differential inductance in Section 3.2. Finally, Section 3.3 derives the online learning rules by embedding the physical constraints into the learning process, thereby enabling online adaptation of the NN.

3.1 Neural network model

Following the general formulation in Patil et al. (2022), a fully-connected feedforward NN with two hidden layers can be modeled as

$$\boldsymbol{\Phi}\left(\boldsymbol{X}_a, \boldsymbol{\theta}\right) := \mathbf{W}_2^\top \boldsymbol{\sigma}_2\left(\mathbf{W}_1^\top \boldsymbol{\sigma}_1\left(\mathbf{W}_0^\top \boldsymbol{X}_a\right)\right), \tag{9}$$

with

$$\boldsymbol{X}_a := \left(\boldsymbol{X}^\top, 1\right)^\top, \quad \boldsymbol{\theta} := \left(\boldsymbol{\theta}_0^\top, \boldsymbol{\theta}_1^\top, \boldsymbol{\theta}_2^\top\right)^\top,$$

where $\boldsymbol{\Phi} : \mathbb{R}^{n_0} \times \mathbb{R}^{n_\theta} \to \mathbb{R}^{n_3}$ is the NN mapping, $\boldsymbol{X}_a \in \mathbb{R}^{n_0}$ is the augmented input with $\boldsymbol{X} \in \mathbb{R}^{n_0-1}$ and a bias term, $\mathbf{W}_j \in \mathbb{R}^{n_j \times n_{j+1}}$ is the weight matrix, and $\boldsymbol{\theta} \in \mathbb{R}^{n_\theta}$ is the vectorized parameter with $\boldsymbol{\theta}_j := \mathrm{vec}(\mathbf{W}_j) \in \mathbb{R}^{n_j n_{j+1}}$ and $n_\theta := \sum_{j=0}^{2} n_j n_{j+1}$. Here, the index $j \in \{0, 1, 2\}$ denotes the layer number, and $n_j \in \mathbb{N}$ denotes the number of nodes within the j^{th} hidden layer, where n_0 and n_3 correspond to the input and output dimensions, respectively. The activation vector $\boldsymbol{\sigma}_j \in \mathbb{R}^{n_j}, \forall j \in \{1, 2\}$ at the hidden layers is defined as

$$\boldsymbol{\sigma}_j := \left(\tanh_{j,1}(\cdot), \ldots, \tanh_{j,n_j-1}(\cdot), 1\right)^\top,$$

where the last node is the bias term and $\tanh_{j,i}(\cdot)$ represents the hyperbolic tangent smooth activation function at the i^{th} node.

The NN model in (9) can be written in a recursive form as

$$\boldsymbol{\Phi}_j := \begin{cases} \mathbf{W}_j^\top \boldsymbol{\sigma}_j\left(\boldsymbol{\Phi}_{j-1}\right), & j \in \{1, 2\} \\ \mathbf{W}_0^\top \boldsymbol{X}, & j = 0 \end{cases} \tag{10}$$

where $\boldsymbol{\Phi}\left(\boldsymbol{X}, \boldsymbol{\theta}\right) = \boldsymbol{\Phi}_2$. This recursive representation is used in the subsequent development of the online physics-informed learning rule.

3.2 NN-based flux and inductance modeling

Using the NN model (9), the solution of the partial differential equation (PDE) (4) (i.e., $\boldsymbol{\psi}_{\mathrm{s}}^{dq}$) can be approximated within a physics-informed learning framework. Accordingly, the flux linkage can be modeled as

$$\boldsymbol{\psi}_{\mathrm{s}}^{dq}(\boldsymbol{i}_{\mathrm{s}}^{dq}) = \boldsymbol{\Phi}(\boldsymbol{x}, \boldsymbol{\theta}^*) + \boldsymbol{\varepsilon}(\boldsymbol{x}), \tag{11}$$

where $\boldsymbol{x} := \left(\boldsymbol{i}_{\mathrm{s}}^{dq\top}, 1\right)^\top \in \mathbb{R}^{n_0}$ denotes the input vector, which can be extended with additional state-dependent terms such as the electrical rotor speed ω_{r}, $\boldsymbol{\varepsilon}(\boldsymbol{x}) \in \mathbb{R}^{n_3}$ is the approximation error with $\|\boldsymbol{\varepsilon}(\boldsymbol{x})\| \le \bar{\varepsilon}$, and $\boldsymbol{\theta}^*$ is the ideal weight vector lying in a compact set with $\|\boldsymbol{\theta}^*\| \le \bar{\theta}$. Then, the approximation of (11) is given by

$$\hat{\boldsymbol{\psi}}_{\mathrm{s}}^{dq}(\boldsymbol{i}_{\mathrm{s}}^{dq}) = \boldsymbol{\Phi}(\boldsymbol{x}, \hat{\boldsymbol{\theta}}), \tag{12}$$

where $\hat{\boldsymbol{\psi}}_{\mathrm{s}}^{dq}$ denotes the estimated flux linkage and $\hat{\boldsymbol{\theta}} \in \mathbb{R}^{n_\theta}$ is the estimated weight parameter.

Applying the chain rule to (12) with respect to the stator current vector $\boldsymbol{i}_{\mathrm{s}}^{dq}$, the estimated differential inductance matrix $\hat{\mathbf{L}}_{\mathrm{s}}^{dq}(\boldsymbol{i}_{\mathrm{s}}^{dq})$ can be modeled as

$$\begin{aligned}\hat{\mathbf{L}}_{\mathrm{s}}^{dq}(\boldsymbol{i}_{\mathrm{s}}^{dq}) &= \nabla_{\boldsymbol{i}_{\mathrm{s}}^{dq}} \boldsymbol{\Phi}\left(\boldsymbol{x}, \hat{\boldsymbol{\theta}}\right) \\ &= \hat{\mathbf{W}}_2^\top \boldsymbol{\sigma}_2'\left(\boldsymbol{\Phi}_1\right) \hat{\mathbf{W}}_1^\top \boldsymbol{\sigma}_1'\left(\boldsymbol{\Phi}_0\right) \hat{\mathbf{W}}_0^\top \frac{\partial \boldsymbol{x}}{\partial \boldsymbol{i}_{\mathrm{s}}^{dq}}\end{aligned} \tag{13}$$

where $\nabla_{\boldsymbol{i}_{\mathrm{s}}^{dq}} \boldsymbol{\Phi}$ denotes the differential inductance Jacobian, $\boldsymbol{\sigma}_j'(\boldsymbol{\Phi}_{j-1}) : \mathbb{R}^{n_j} \to \mathbb{R}^{n_j \times n_j}$ denotes the activation Jacobian defined by $\boldsymbol{\sigma}_j'(y) = \frac{\partial}{\partial z} \boldsymbol{\sigma}_j(z)\big|_{z=y}$ for $j \in \{1, 2\}$, and $\frac{\partial \mathbf{x}}{\partial \boldsymbol{i}_{\mathrm{s}}^{dq}} \in \mathbb{R}^{n_0 \times 2}$ is the Jacobian of the augmented input vector with respect to the current vector.

3.3 Online physics-informed learning rules

Using (12) and (13), the flux linkage and differential inductance approximated by the NN are constrained by the governing PDE (4), and the corresponding residual is defined as

$$\begin{aligned}\mathcal{R}\left(\boldsymbol{x}, \hat{\boldsymbol{\theta}}\right) :=& \nabla_{\boldsymbol{i}_{\mathrm{s}}^{dq}} \boldsymbol{\Phi}\left(\boldsymbol{x}, \hat{\boldsymbol{\theta}}\right) \frac{\mathrm{d}}{\mathrm{d}t} \boldsymbol{i}_{\mathrm{s}}^{dq} - \left(\boldsymbol{v}_{\mathrm{s}}^{dq} - \mathrm{R}_{\mathrm{s}} \boldsymbol{i}_{\mathrm{s}}^{dq}\right. \\ &\left. - \omega_{\mathrm{r}} \mathbf{J} \boldsymbol{\Phi}\left(\boldsymbol{x}, \hat{\boldsymbol{\theta}}\right)\right),\end{aligned} \tag{14}$$

where $\mathcal{R} \in \mathbb{R}^{n_3}$ denotes the predicted residual vector, reflecting the governing dynamics of SM. The objective is to find the optimal weight vector $\hat{\boldsymbol{\theta}}^*$ that minimizes the residual for any $\boldsymbol{x}$. To quantify this residual minimization, the loss function $\mathcal{L} : \mathbb{R}^{n_\theta} \to \mathbb{R}_{\ge 0}$ is defined as

$$\mathcal{L}\left(\boldsymbol{x}, \hat{\boldsymbol{\theta}}\right) := \frac{1}{2} \left\|\mathcal{R}\left(\boldsymbol{x}, \hat{\boldsymbol{\theta}}\right)\right\|^2, \tag{15}$$

Table 1. Specifications of the IPMSM.

Parameter	Value
Rated mech. power	35 kW
Rated mech. speed	2000 RPM
Rated mech. torque	180 Nm
Max. stator voltage (v_s)	160 V
Max. stator current (i_s)	350 A
Pole pairs (P)	8
Stator resistance ($\mathrm{R_s}$)	10.7 mΩ

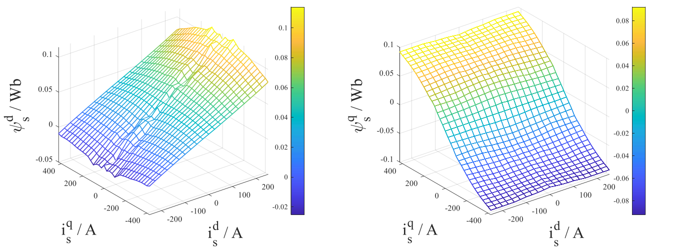

(a) (b)

Fig. 1. Stator flux linkage maps corresponding to the d-axis (a) and q-axis (b).

where the corresponding residual minimization problem is formulated through a gradient-based learning rule given by

$$\begin{aligned}\dot{\hat{\boldsymbol{\theta}}} &= -\Gamma \nabla_{\hat{\boldsymbol{\theta}}} \mathcal{L}(\boldsymbol{x}, \hat{\boldsymbol{\theta}}) \\ &= -\Gamma \left(\nabla_{\hat{\boldsymbol{\theta}}} \left(\nabla_{\boldsymbol{i}_\mathrm{s}^{dq}} \boldsymbol{\Phi}(\boldsymbol{x}, \hat{\boldsymbol{\theta}}) \frac{\mathrm{d}}{\mathrm{d}t} \boldsymbol{i}_\mathrm{s}^{dq} \right) \right. \\ &\qquad \left. + \ \omega_\mathrm{r} \mathbf{J} \, \nabla_{\hat{\boldsymbol{\theta}}} \boldsymbol{\Phi}(\boldsymbol{x}, \hat{\boldsymbol{\theta}}) \right)^\top \mathcal{R}(\boldsymbol{x}, \hat{\boldsymbol{\theta}}), \qquad (16)\end{aligned}$$

where $\Gamma \in \mathbb{R}^{n_\theta \times n_\theta}$ is the postive-definite learning rate and $\nabla_{\hat{\boldsymbol{\theta}}} \boldsymbol{\Phi}(\boldsymbol{x}, \hat{\boldsymbol{\theta}}) := \left[\frac{\partial \boldsymbol{\Phi}_0}{\partial \boldsymbol{\theta}_0}, \frac{\partial \boldsymbol{\Phi}_1}{\partial \boldsymbol{\theta}_1}, \frac{\partial \boldsymbol{\Phi}_2}{\partial \boldsymbol{\theta}_2} \right] \in \mathbb{R}^{n_3 \times n_\theta}$ is the Jacobian of the feedforward NN with respect to the weight vector and can be computed by the chain rule and vectorized backpropagation. The term $\nabla_{\hat{\boldsymbol{\theta}}} \left(\nabla_{\boldsymbol{i}_\mathrm{s}^{dq}} \boldsymbol{\Phi}(\boldsymbol{x}, \hat{\boldsymbol{\theta}}) \frac{\mathrm{d}}{\mathrm{d}t} \boldsymbol{i}_\mathrm{s}^{dq} \right)$ contains mixed second–order derivatives of $\boldsymbol{\Phi}$ with respect to $(\boldsymbol{i}_\mathrm{s}^{dq}, \hat{\boldsymbol{\theta}})$, i.e., Hessian–vector products. Note that the time derivative $\frac{\mathrm{d}}{\mathrm{d}t} \boldsymbol{i}_\mathrm{s}^{dq}$ can be approximated in discrete time using the forward Euler method as $\frac{\mathrm{d}}{\mathrm{d}t} \boldsymbol{i}_\mathrm{s}^{dq} \approx (\boldsymbol{i}_{\mathrm{s},k}^{dq} - \boldsymbol{i}_{\mathrm{s},k-1}^{dq})/T_\mathrm{s}$, where T_s denotes the sampling period and k is the discrete-time index.

4. SIMULATION VALIDATION

The proposed online physics-informed flux model learning was validated using MATLAB & Simulink R2024b. The simulation environment was constructed based on the `Three-Phase PMSM Traction Drive` example, which includes a high-fidelity 35 kW interior permanent magnet synchronous machine (IPMSM) drive model provided by MathWorks. The key specifications of the IPMSM are summarized in Table 1, and the two-dimensional lookup tables for the flux linkage maps used in this model are illustrated in Fig. 1.

This section consisted of two parts, focusing on (i) assessing the estimation performance of the flux linkages obtained from the online learning model, and (ii) examining the effectiveness of applying the learned parameters to the online MTPA control. In the first part, the NN-based flux–inductance model learned online was used directly as an estimator, and its performance was analyzed by comparing it with a LUT-based flux model at a fixed mechanical speed of 500 RPM over a wide operating range (torque 0–180 Nm with a 50 Hz bandwidth). For the second part, the online-learned parameters (i.e., flux linkages and differential inductances) were applied to the MTPA control law in (7), and the resulting performance was compared against a LUT-based baseline method and a DOBFLE–RLS-based method, which estimates the flux linkage using DOBFLE and identifies the differential inductances via RLS. The details of each method are described below.

1) LUT-based MTPA: A two-dimensional flux linkage lookup table parameterized through intensive experiments and FEM analysis was used as the baseline flux model. Based on these flux maps, the MTPA trajectories were computed by applying the numerical technique presented in Choi et al. (2021).

2) DOBFLE–RLS-based MTPA: The DOBFLE described in Monzen et al. (2023) is a state-of-the-art flux estimator that decomposes the stator flux linkage into linear and nonlinear disturbance components and models them as observer states. To ensure reliable estimation performance, the observer gain matrix was designed following the guidelines in Jang et al. (2025) to achieve an observer bandwidth of 100 Hz. Given the flux estimate $\hat{\boldsymbol{\psi}}_\mathrm{s}^{dq}$ from DOBFLE, the differential inductances were computed in discrete time using an RLS formulation following Varatharajan et al. (2017), expressed as

$$\hat{\mathbf{L}}_{\mathrm{s},k}^{dq} \Delta \boldsymbol{i}_{\mathrm{s},k}^{dq} = T_\mathrm{s} \left(\boldsymbol{v}_{\mathrm{s},k-1}^{dq} - \mathrm{R_s} \boldsymbol{i}_{\mathrm{s},k-1}^{dq} - \omega_{\mathrm{s},k-1} \mathbf{J} \hat{\boldsymbol{\psi}}_{\mathrm{s},k-1}^{dq} \right), \qquad (17)$$

where $\Delta \boldsymbol{i}_{\mathrm{s},k}^{dq} := \boldsymbol{i}_{\mathrm{s},k}^{dq} - \boldsymbol{i}_{\mathrm{s},k-1}^{dq}$. Equation (17) serves as the regression model used in the RLS update, for which a forgetting factor of 0.999 and an initial covariance matrix of $\mathbf{P}_0 = 10^{-4} \mathbf{I}_4$ were used. Accordingly, the resulting flux and inductance estimates were incorporated into the MTPA control law in (7) to compute the gradient terms required for the online MTPA operation.

3) Proposed Method (PM): For the proposed approach, the NN model in (9) was configured with hyperparameters $n_0 = 3$, $n_1 = 5$, $n_2 = 5$, and $n_3 = 2$. The learning rates in (16) were set differently across layers: 30 for the output layer ($j = 2$) and 5×10^{-3} for the hidden and input layers ($j = 1, 0$), respectively. The sampling time was chosen as $T_\mathrm{s} = 5 \times 10^{-5}$ s (20 kHz). The initial NN weights were randomly initialized such that the resulting initial differential inductance matrix matched $\mathbf{L}_{\mathrm{s},0} := \begin{bmatrix} 0.24 & 0.01 \\ 0.01 & 0.32 \end{bmatrix}$ mH. Similar to the DOBFLE–RLS-based approach, the MTPA control law in (7) was executed online using the flux and differential inductance estimates learned by the NN.

4.1 Validation of estimation performance

Figure 2 illustrates the estimation performance of the flux linkages and differential inductances learned by the proposed online physics-informed model learning framework

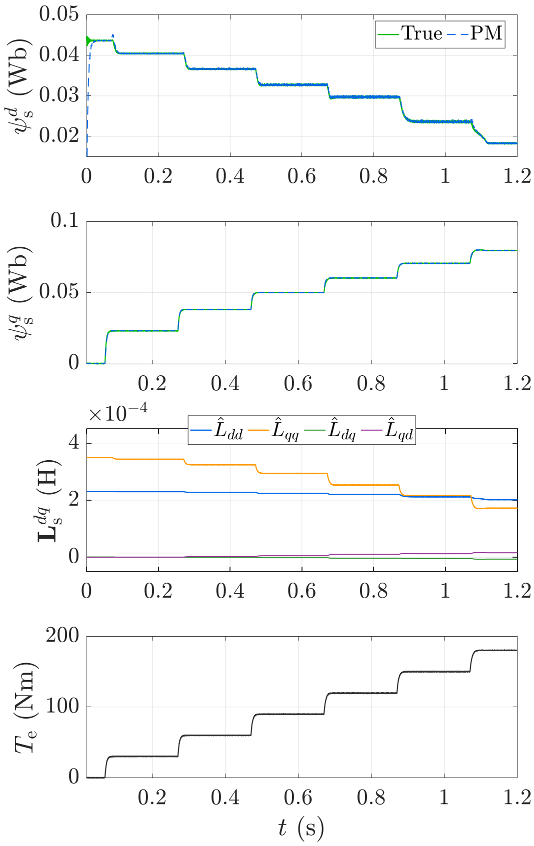

Fig. 2. Stator flux linkage and differential inductance estimates from the proposed method (PM) under varying torque commands conditions at a fixed mechanical speed of 500 RPM.

under torque variations from 0 to 180 Nm at a fixed mechanical speed of 500 RPM. During the learning phase, the torque $\mathrm{T_e}$ is increased from 0 Nm to 180 Nm with a 50 Hz bandwidth, using 30 Nm step increments every 0.2 s interval, and reaches its maximum value at $t = 1.1$ s.

At the beginning of the learning process, the initial differential inductance weights were selected with values that deviate from the true differential inductances, causing the flux estimates—particularly on the d–axis—to exhibit spike–like errors at around $t = 0.1$ s. However, once the online learning continues, the estimated flux rapidly converges to the true value, indicating that the neural network weights are continuously updated at each step toward a locally optimal solution that minimizes the residuals predicted by the NN model.

During the identification process, the flux and inductance models are updated simultaneously online according to the learning rule (16). As shown in Fig. 2, the differential inductances vary in accordance with the flux estimation. In particular, after $t = 0.7$ s (i.e., when T_e exceeds approximately 120 Nm), the influence of the cross-coupling terms $\hat{L}_s^{dq}$ and $\hat{L}_s^{qd}$ becomes more significant as the torque increases. Consequently, the self-differential inductances $\hat{L}_s^{dd}$ and $\hat{L}_s^{qq}$ exhibit a decreasing trend as the torque increases.

4.2 Comparison of MTPA control performance

The effectiveness of the MTPA control in (7) under the proposed method and the DOBFLE–RLS was evaluated by comparing their d- and q-axis stator current trajectories and the corresponding copper losses against those of the LUT-based MTPA control, as shown in Fig. 3. As in Section 4.1, the simulation scenario involved varying the torque command $\mathrm{T_e^*}$ from 0 Nm to 180 Nm with a 50 Hz bandwidth, while the mechanical speed was kept constant at 500 RPM.

Figure 3a shows that in the low-torque region around $\mathrm{T_e} = 60$ Nm, the current trajectories of both methods are comparable to those obtained with the LUT-based MTPA method. However, as the torque command increases, the DOBFLE-RLS-based method exhibits a noticeable deviation from the LUT-based reference, particularly in the d-axis current trajectory. At $\mathrm{T_e} = 90$ Nm, Figure 3b shows a maximum copper loss increase of 55.93% compared with the LUT-based MTPA method, indicating a significant degradation in torque generation accuracy, which consequently leads to suboptimal copper loss minimization. This degradation is primarily attributed to numerical noise arising from the incremental variations $\Delta\psi_{\mathrm{s},k}^{dq}$ and $\Delta i_{\mathrm{s},k}^{dq}$, despite the superior flux estimation capability of DOBFLE.

In contrast, the proposed method consistently provides accurate current trajectories that closely follow those of the LUT-based MTPA trajectory. This improved performance arises from the online physics-informed model learning framework, which enables the NN to learn the flux and inductance models directly from the underlying physical behavior of the SM. As a result, the proposed method accurately estimates the parameters required for MTPA control through the NN-based online learning framework. Consequently, it achieves a maximum copper loss of only 0.79% at $\mathrm{T_e} = 180$ Nm, demonstrating its effectiveness in maintaining accurate torque generation.

5. CONCLUSION

An online physics-informed learning framework is proposed, in which the physical laws of synchronous machines are directly embedded into the learning process. The proposed method enables a fully connected feedforward NN to model the nonlinear flux linkages and differential inductances and to learn them online under the constraints imposed by the governing equations of the SMs. By doing so, the proposed approach enables the online estimation of the flux linkages and differential inductances required for MTPA control. The effectiveness of the proposed method was validated through simulations on a 35-kW IPMSM drive, and its performance was evaluated by comparison with the DOBFLE–RLS-based method and a LUT-based MTPA baseline.

Future work includes extending the online physics-informed learning framework by leveraging data acquired from a wide range of operating conditions to improve global learning performance, as well as conducting experimental validation to demonstrate the practical applicability of the proposed method.

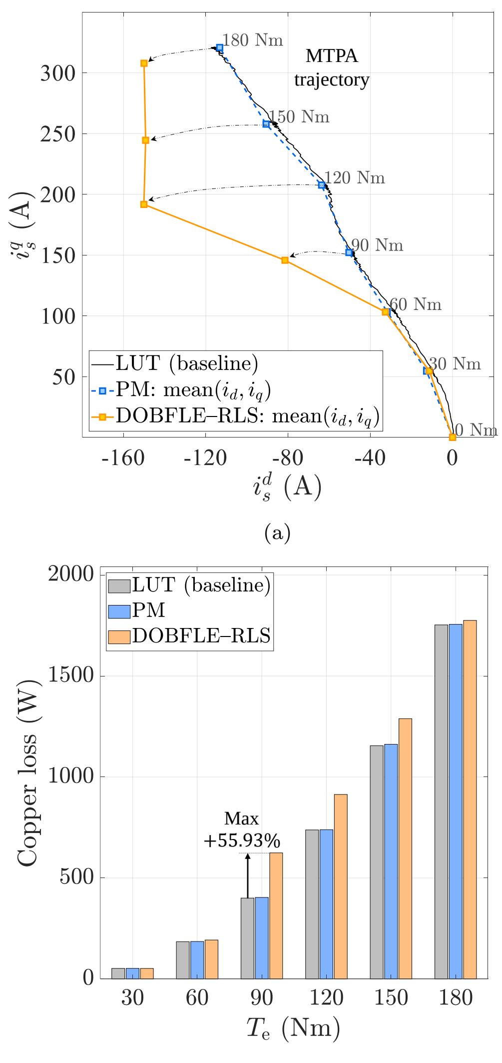

Fig. 3. Comparison of the proposed method and the DOBFLE-RLS-based method against the LUT-based MTPA trajectroy: (a) d- and q-axis current trajectories, and (b) copper-loss.

REFERENCES

Ahmed, A.A., Kwon Koh, B., Kim, J.S., and Il Lee, Y. (2017). Finite control set-model predictive speed control for induction motors with optimal duration. *IFAC-PapersOnLine*, 50(1), 7801–7806. 20th IFAC World Congress.

Brosch, A., Wallscheid, O., and Böcker, J. (2021). Torque and inductances estimation for finite model predictive control of highly utilized permanent magnet synchronous motors. *IEEE Transactions on Industrial Informatics*, 17(12), 8080–8091. doi:10.1109/TII.2021.3060469.

Choi, K., Kim, J., and Park, K.B. (2025). Generalized model predictive torque control of synchronous machines. *IEEE/ASME Transactions on Mechatronics*, 30(4), 2643–2653. doi:10.1109/TMECH.2024.3461209.

Choi, K., Kim, Y., Kim, K.S., and Kim, S.K. (2021). Real-time optimal torque control of interior permanent magnet synchronous motors based on a numerical optimization technique. *IEEE Transactions on Control Systems Technology*, 29(4), 1815–1822. doi:10.1109/TCST.2020.3006900.

Jang, S. and Choi, K. (2023). Stator flux linkage estimation of synchronous machines based on integration error estimation for improved transient performance. In *2023 62nd IEEE Conference on Decision and Control (CDC)*, 4197–4202. doi:10.1109/CDC49753.2023.10383827.

Jang, S., Pfeifer, B., Hackl, C.M., and Choi, K. (2024). Extended state observer based stator flux linkage estimation of nonlinear synchronous machines. In *2024 IEEE 33rd International Symposium on Industrial Electronics (ISIE)*, 1–5. IEEE.

Jang, S., Ryu, M., and Choi, K. (2025). Physics-informed online learning of flux linkage model for synchronous machines. In *IECON 2025 – 51st Annual Conference of the IEEE Industrial Electronics Society*, 1–6. doi:10.1109/IECON58223.2025.11221587.

Lee, J.S., Choi, C.H., Seok, J.K., and Lorenz, R.D. (2011). Deadbeat-direct torque and flux control of interior permanent magnet synchronous machines with discrete time stator current and stator flux linkage observer. *IEEE Transactions on Industry Applications*, 47(4), 1749–1758. doi:10.1109/TIA.2011.2154293.

Monzen, N. and Hackl, C.M. (2025). Optimal reference voltage saturation for nonlinear current control of synchronous machine drives. *IEEE Transactions on Industry Applications*, 1–10. doi:10.1109/TIA.2025.3589967.

Monzen, N., Pfeifer, B., and Hackl, C.M. (2023). A simple disturbance observer for stator flux linkage estimation of nonlinear synchronous machines. In *2023 IEEE 32nd International Symposium on Industrial Electronics (ISIE)*, 1–6. doi:10.1109/ISIE51358.2023.10227965.

Ortombina, L., Tinazzi, F., and Zigliotto, M. (2019). Adaptive maximum torque per ampere control of synchronous reluctance motors by radial basis function networks. *IEEE Journal of Emerging and Selected Topics in Power Electronics*, 7(4), 2531–2539. doi:10.1109/JESTPE.2018.2858842.

Patil, O.S., Le, D.M., Greene, M.L., and Dixon, W.E. (2022). Lyapunov-derived control and adaptive update laws for inner and outer layer weights of a deep neural network. *IEEE Control Systems Letters*, 6, 1855–1860. doi:10.1109/LCSYS.2021.3134914.

Rodriguez, J., Garcia, C., Mora, A., Flores-Bahamonde, F., Acuna, P., Novak, M., Zhang, Y., Tarisciotti, L., Davari, S.A., Zhang, Z., Wang, F., Norambuena, M., Dragicevic, T., Blaabjerg, F., Geyer, T., Kennel, R., Khaburi, D.A., Abdelrahem, M., Zhang, Z., Mijatovic, N., and Aguilera, R.P. (2022). Latest advances of model predictive control in electrical drives—part i: Basic concepts and advanced strategies. *IEEE Transactions on Power Electronics*, 37(4), 3927–3942. doi:10.1109/TPEL.2021.3121532.

Varatharajan, A., Cruz, S., Hadla, H., and Briz, F. (2017). Predictive torque control of synrm drives with online mtpa trajectory tracking and inductances estimation. In *2017 IEEE International Electric Machines and Drives Conference (IEMDC)*, 1–7. doi:10.1109/IEMDC.2017.8002104.

Yoo, A. and Sul, S.K. (2009). Design of flux observer robust to interior permanent-magnet synchronous motor flux variation. *IEEE Transactions on Industry Applications*, 45(5), 1670–1677. doi:10.1109/TIA.2009.2027516.